

Controlling Spin Exchange Interactions of Ultracold Atoms in Optical Lattices

L.-M. Duan,¹ E. Demler,² and M. D. Lukin²

¹*Institute for Quantum Information, California Institute of Technology, mc 107-81, Pasadena, California 91125, USA*

²*Physics Department, Harvard University, Cambridge, Massachusetts 02138, USA*

(Received 25 October 2002; published 26 August 2003)

We describe a general technique that allows one to induce and control strong interaction between spin states of neighboring atoms in an optical lattice. We show that the properties of spin exchange interactions, such as magnitude, sign, and anisotropy, can be designed by adjusting the optical potentials. We illustrate how this technique can be used to efficiently “engineer” quantum spin systems with desired properties, for specific examples ranging from scalable quantum computation to probing a model with complex topological order that supports exotic anyonic excitations.

DOI: 10.1103/PhysRevLett.91.090402

PACS numbers: 03.75.Nt, 03.67.-a, 42.50.-p, 73.43.-f

Recent observations of the superfluid to Mott insulator transition in a system of ultracold atoms in an optical lattice open fascinating prospects for studying many-body phenomena associated with strongly correlated systems in a highly controllable environment [1–4]. For instance, the recent studies have shown that, with spinor bosonic or fermionic atoms in optical lattices, it may be possible to observe complex quantum phase transitions [5,6], to probe novel superfluidity mechanisms [7,8], or to demonstrate the spin-charge separation predicted from the Luttinger liquid model [9].

This Letter describes a general technique to control many-body spin Hamiltonians using ultracold atoms. Specifically, we show that, when two-state bosonic or fermionic atoms are confined in an optical lattice, the interaction between spins of the particles can be controlled by adjusting the intensity, frequency, and polarization of the trapping light. The essential idea is to induce and control virtual spin-dependent tunneling between neighboring atoms in the lattice that results in a controllable Heisenberg exchange interaction. By combining this simple experimental technique with the design of the lattice geometry, it is possible to engineer many interesting spin Hamiltonians corresponding to strongly correlated systems.

Such techniques are of particular significance since quantum magnetic interactions are central to understanding complex orders and correlations [10]. We illustrate this with several examples: (i) We show that one of the generated Hamiltonians provides us an easy way to realize the so-called cluster states in two or three dimensions [11], which are useful for an implementation of scalable quantum computation with neutral atoms; (ii) we show that the realized Hamiltonian has a rich phase diagram, opening up the possibility to observe various quantum magnetic phase transitions in a controllable way; (iii) finally, we show how to implement an exactly solvable spin Hamiltonian recently proposed by Kitaev [12], which supports Abelian and non-Abelian anyonic excitations with exotic fractional statistics. Abelian anyons could also exist in a fast rotating condensate [13].

We consider an ensemble of ultracold bosonic or fermionic atoms confined in an optical lattice formed by several standing-wave laser beams. We are interested in the Mott insulator regime, and the atomic density of roughly one atom per lattice site. Each atom is assumed to have two relevant internal states, which are denoted with the effective spin index $\sigma = \uparrow, \downarrow$, respectively. We assume that the atoms with spins $\sigma = \uparrow, \downarrow$ are trapped by independent standing-wave laser beams through polarization (or frequency) selection. Each laser beam creates a periodic potential $V_{\mu\sigma} \sin^2(\vec{k}_\mu \cdot \vec{r})$ in a certain direction μ , where \vec{k}_μ is the wave vector of light. For sufficiently strong periodic potential and low temperatures, the atoms will be confined to the lowest Bloch band as has been confirmed from experiments [1], and the low energy Hamiltonian is then given by

$$H = - \sum_{\langle ij \rangle \sigma} (t_{\mu\sigma} a_{i\sigma}^\dagger a_{j\sigma} + \text{H.c.}) + \frac{1}{2} \sum_{i\sigma} U_\sigma n_{i\sigma} (n_{i\sigma} - 1) + U_{\uparrow\downarrow} \sum_i n_{i\uparrow} n_{i\downarrow}, \quad (1)$$

Here $\langle i, j \rangle$ denotes the near neighbor sites in the direction μ , $a_{i\sigma}$ are bosonic (or fermionic) annihilation operators, respectively, for bosonic (or fermionic) atoms of spin σ localized on-site i , and $n_{i\sigma} = a_{i\sigma}^\dagger a_{i\sigma}$.

For the cubic lattice ($\mu = x, y, z$) and using a harmonic approximation around the minima of the potential [3], the spin-dependent tunneling energies and the on-site interaction energies are given by $t_{\mu\sigma} \approx (4/\sqrt{\pi}) E_R^{1/4} (V_{\mu\sigma})^{3/4} \times \exp[-2(V_{\mu\sigma}/E_R)^{1/2}]$, $U_{\uparrow\downarrow} \approx (8/\pi)^{1/2} (ka_{s\uparrow\downarrow}) \times (E_R \bar{V}_{1\uparrow\downarrow} \bar{V}_{2\uparrow\downarrow} \bar{V}_{3\uparrow\downarrow})^{1/4}$. Here $\bar{V}_{\mu\uparrow\downarrow} = 4V_{\mu\uparrow} V_{\mu\downarrow} / (V_{\mu\uparrow}^{1/2} + V_{\mu\downarrow}^{1/2})^2$ is the spin average potential in each direction, $E_R = \hbar^2 k^2 / 2m$ is the atomic recoil energy, and $a_{s\uparrow\downarrow}$ is the scattering length between the atoms of different spins. For bosonic atoms $U_\sigma \approx (8/\pi)^{1/2} (ka_{s\sigma}) (E_R V_{1\sigma} V_{2\sigma} V_{3\sigma})^{1/4}$ ($a_{s\sigma}$ are the corresponding scattering lengths). For fermionic atoms, U_σ is on the order of Bloch band separation $\sim 2\sqrt{V_{\mu\sigma} E_R}$, which is typically much larger than $U_{\uparrow\downarrow}$ and can be taken to be infinite. In writing Eq. (1), we have neglected overall energy shifts $\sum_{i\mu} (\sqrt{E_R V_{\mu\uparrow}} - \sqrt{E_R V_{\mu\downarrow}}) (n_{i\uparrow} - n_{i\downarrow}) / 2$, which can be easily compensated

by a homogeneous external magnetic field applied in the z direction.

From the above expressions, we observe that $t_{\mu\sigma}$ depend sensitively (exponentially) upon the ratios $V_{\mu\sigma}/E_R$, while U_{\parallel} and U_{σ} exhibit only weak dependence. We can easily introduce spin-dependent tunneling $t_{\mu\sigma}$ by varying the potential depth $V_{\mu\uparrow}$ and $V_{\mu\downarrow}$ with control of the intensity of the trapping laser. We now show that this simple experimental method provides us a powerful tool to engineer many-body Hamiltonians. We are interested in the regime where $t_{\mu\sigma} \ll U_{\sigma}, U_{\parallel}$ and $\langle n_{i\uparrow} \rangle + \langle n_{i\downarrow} \rangle \simeq 1$, which corresponds to an insulating phase. In this regime, the terms proportional to tunneling $t_{\mu\sigma}$ can be considered via perturbation theory. We use a simple generalization of the Schrieffer-Wolf transformation [14] (see another method in [8]) and, to the leading order in $t_{\mu\sigma}/U_{\parallel}$, Eq. (1) is equivalent to the following effective Hamiltonian:

$$H = \sum_{\langle i,j \rangle} [\lambda_{\mu z} \sigma_i^z \sigma_j^z \pm \lambda_{\mu\perp} (\sigma_i^x \sigma_j^x + \sigma_i^y \sigma_j^y)]. \quad (2)$$

Here $\sigma_i^z = n_{i\uparrow} - n_{i\downarrow}$, $\sigma_i^x = a_{i\uparrow}^\dagger a_{i\downarrow} + a_{i\downarrow}^\dagger a_{i\uparrow}$, and $\sigma_i^y = -i(a_{i\uparrow}^\dagger a_{i\downarrow} - a_{i\downarrow}^\dagger a_{i\uparrow})$ are the usual spin operators. The + and - signs before $\lambda_{\mu\perp}$ in Eq. (4) correspond, respectively, to the cases of fermionic and bosonic atoms. The parameters $\lambda_{\mu z}$ and $\lambda_{\mu\perp}$ for the bosonic atoms are given by

$$\lambda_{\mu z} = \frac{t_{\mu\uparrow}^2 + t_{\mu\downarrow}^2}{2U_{\parallel}} - \frac{t_{\mu\uparrow}^2}{U_{\uparrow}} - \frac{t_{\mu\downarrow}^2}{U_{\downarrow}}, \quad \lambda_{\mu\perp} = \frac{t_{\mu\uparrow} t_{\mu\downarrow}}{U_{\parallel}}. \quad (3)$$

For fermionic atoms, the expression for λ_{\perp} is the same as in (3), but in the expression for λ_z the last two terms vanish since $U_{\sigma} \gg U_{\parallel}$. In writing Eq. (2), we neglected the term $\sum_{i\mu} 4(t_{\mu\uparrow}^2/U_{\uparrow} - t_{\mu\downarrow}^2/U_{\downarrow})\sigma_i^z$, which can be easily compensated by an applied external magnetic field.

The Hamiltonian (2) represents the well-known anisotropic Heisenberg model (XXZ model), which arises in the context of various condensed matter systems [10]. However, the approach involving ultracold atoms has a unique advantage in that the parameters $\lambda_{\mu z}$ and $\lambda_{\mu\perp}$ can be easily controlled by adjusting the intensity of the trapping laser beams. They can also be changed within a broad range by tuning the ratio between the scattering lengths $a_{s\uparrow}$ and $a_{s\sigma}$ ($\sigma = \uparrow, \downarrow$) by adjusting an external magnetic field through Feshbach resonance [15]. Therefore, even with bosonic atoms alone, it is possible to realize the entire class of Hamiltonians in the general form (2) with an arbitrary ratio $\lambda_{\mu z}/\lambda_{\mu\perp}$. This is important since bosonic atoms are generally easier to cool. In Fig. 1(a), we show the phase diagram of the Hamiltonian (2) on a bipartite lattice as a function of $\beta_t = t_{\uparrow}/t_{\downarrow} + t_{\downarrow}/t_{\uparrow}$ and U_{\parallel}/U_{σ} [16] for the case when $U_{\uparrow} = U_{\downarrow}$ and $t_{\mu\sigma}$ is independent of the spatial direction μ . Certain lines on this phase diagram correspond to well-known spin systems: When $U_{\parallel}/U_{\sigma} = 1/2$ we have an XY model; when $\beta_t = \infty$ (t_{\uparrow} or t_{\downarrow} is zero) we have an Ising model; for $\beta_t =$

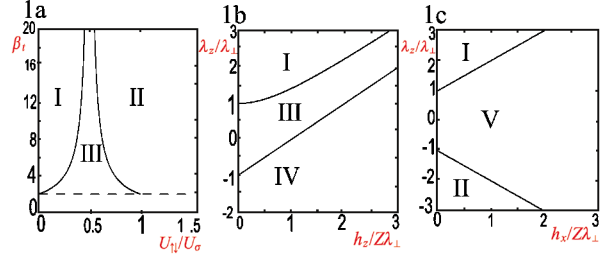


FIG. 1 (color online). Phase diagrams of the Hamiltonians (2) for bosonic and fermionic atoms: (a) at zero magnetic field, (b) with a longitudinal field h_z , and (c) (for bosons only) with a transverse field h_x . Each phase is characterized by the following order parameter: I, z -Néel order; II, z -ferromagnetic order; III, xy -Néel order for fermionic atoms and xy -ferromagnetic order for bosonic atoms; IV and V, spin polarization in the direction of applied field, z and x , respectively.

$\pm(1/2 - U_{\parallel}/U_{\sigma})^{-1}$ we have an SU(2) symmetric anti-ferromagnetic or ferromagnetic systems, respectively.

Before proceeding, we estimate the typical energy scales and discuss the influence of imperfections and noise. For Rb atoms with a lattice constant $\pi/|k| \sim 426$ nm, the typical tunneling rate t/\hbar can be chosen from zero to a few kHz [1]. The on-site interaction U/\hbar corresponds to a few kHz at zero magnetic field, but can be much larger near the Feshbach resonance. The energy scale for magnetic interaction is about $t^2/\hbar U \sim 0.1$ kHz (corresponding to a time scale of 10 ms) with a conservative choice of $U \sim 2$ kHz and $(t/U)^2 \sim 1/20$. These energy scales are clearly compatible with current experiments [1]. We further note that the present system should be quite robust to realistic noise and imperfections. First of all, the next order correction to the Hamiltonian (2) is proportional to $(t/U)^2$, which is small in the Mott regime. Second, since the atoms only virtually tunnel to the neighboring sites with a small probability $(t/U)^2$, the dephasing rate and the inelastic decay rate are significantly reduced compared with the cold collision scheme [17,18]. Finally, the spontaneous emission noise rate can be made very small by using a blue-detuned optical lattice or by increasing the detuning. In a blue-detuned lattice, even with a moderate detuning $\Delta \sim 5$ GHz, the effective spontaneous emission rate is estimated to be of the order of Hz, which is significantly smaller than $t^2/(\hbar U)$.

We now illustrate the ability to engineer many-body spin Hamiltonians with specific examples. For the first example, we set $V_{\mu\downarrow}/V_{\mu\uparrow} \gg 1$, so that $t_{\mu\downarrow}$ becomes negligible while $t_{\mu\uparrow}$ remains finite. In this case, the Hamiltonian (2) reduces to the Ising model $H = \sum_{\langle i,j \rangle} \lambda_{\mu z} \sigma_i^z \sigma_j^z$, with $\lambda_{\mu z} = t_{\mu\uparrow}^2/(0.5/U_{\parallel} - 1/U_{\uparrow})$. Though this Hamiltonian has quite trivial properties for its ground states and excitations, its realization in optical lattices can be very useful for a dynamical generation of the so-called cluster states [11]. Specifically, we note that this Ising interaction can be easily turned on and off by adjusting the potential depth $V_{\mu\uparrow}$. If we first prepare each atom in the lattice into the superposition state $(|\uparrow\rangle + |\downarrow\rangle)/\sqrt{2}$, and

then lower $V_{\mu\uparrow}$ for a time T with $\lambda_{\mu z}T = \pi/4 \bmod \pi/2$, the final state is a cluster state with its dimension determined by the dimension of the lattice [11]. The d -dimensional ($d \geq 2$) cluster states have important applications for implementation of scalable quantum computation with neutral atoms: After its preparation, one can implement universal quantum computation simply via a series of single-bit measurements only [11]. The use of such cluster states can significantly alleviate the stringent requirements on separate addressing of the neighboring atoms in the proposed quantum computation schemes [17,19]. Although the present approach is somewhat slower than the cold collision scheme [17], it allows one to take advantage of its simplicity and the reduced dephasing rate.

As our second example, we explore the rich phase diagram of the Hamiltonian (2) in the presence of magnetic fields. For simplicity, we assume a bipartite lattice and identical spin exchange constants for all links. Figure 1(b) shows the mean-field phase diagram for bosonic particles in the presence of a longitudinal field h_z . This diagram was obtained by comparing energies of the variational wave functions of two kinds: (i) the Néel state in the z direction $\langle \vec{\sigma}_i \rangle = (-1)^i \vec{e}_z$; (ii) canted phase with ferromagnetic order in the xy plane and finite polarization in the z direction $\langle \vec{\sigma}_i \rangle = \vec{e}_x \cos\theta + \vec{e}_z \sin\theta$. Here, θ is a variational parameter, and $\vec{e}_{z,x}$ are unit vectors in the directions z, x . Transition between the z -Néel and the canted phases is a first order spin-flop transition [20] at $h_z = Z(\lambda_z^2 - \lambda_\perp^2)^{1/2}$ (Z is the number of neighboring atoms of each lattice site), and transition between the xy -Néel phase and the z polarized phase is a second order transition of the XY type at $h_z = Z(\lambda_z + \lambda_\perp)$. In the absence of transverse magnetic field, one can use the existence of two sublattices to change the sign of λ_\perp using the transformation $\sigma_i^{x,y} \rightarrow (-1)^i \sigma_i^{x,y}$. Hence, fermionic atoms in the longitudinal magnetic field have the same phase diagram as shown in Fig. 1(b), except that their canted phase has transverse Néel rather than transverse ferromagnetic order. Results of a similar mean-field analysis of the Hamiltonian (2) for bosonic atoms with a transverse magnetic field h_x are shown in Fig. 1(c). For fermionic atoms in a transverse field, there is one more phase with a Néel order along y direction.

The third example involves the anisotropic spin model on a 2D hexagonal lattice proposed recently by Kitaev [12]. In this model, interactions between nearest neighbors are of the XX , the YY , or the ZZ type, depending on the direction of the link:

$$H = \sum_{\nu=x,y,z; \langle i,j \rangle \in D_\nu} \lambda_\nu \sigma_i^\nu \sigma_j^\nu, \quad (4)$$

where the symbol $\langle i, j \rangle \in D_\nu$ denotes the neighboring atoms in the D_ν ($\nu = x, y, z$) direction [see Fig. 2(b)].

To implement this model using ultracold atoms, we first raise the potential barriers along the vertical direction Z

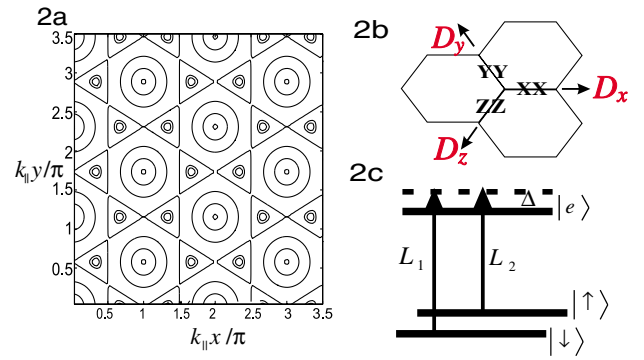


FIG. 2 (color online). (a) The contours with the three potentials in the form of Eq. (5). The minima are at the centers of the triangles when $\varphi_0 = \pi/2$. (b) The illustration of the model Hamiltonian (4). (c) The schematic atomic level structure and the laser configuration to induce spin-dependent tunneling.

in the three-dimensional optical lattice so that the tunneling and the spin exchange interactions in Z direction are completely suppressed [1,9]. In this way, we get an effective 2D configuration with a set of independent identical 2D lattice in the X - Y plane. We then apply in the X - Y plane three trapping potentials (identical for all spin states) of the forms

$$V_j(x, y) = V_0 \sin^2[k_\parallel(x \cos\theta_j + y \sin\theta_j) + \varphi_0], \quad (5)$$

where $j = 1, 2, 3$, and $\theta_1 = \pi/6$, $\theta_2 = \pi/2$, $\theta_3 = -\pi/6$. Each of the potentials is formed by two blue-detuned interfering traveling laser beams above the X - Y plane with an angle $\varphi_\parallel = 2 \arcsin(1/\sqrt{3})$, so that the wave vector k_\parallel projected onto the X - Y plane has the value $k_\parallel = k \sin(\varphi_\parallel/2) = k/\sqrt{3}$. We choose the relative phase $\varphi_0 = \pi/2$ in Eq. (5) so that the maxima of the three potentials overlap. In this case, the atoms are trapped at the minima of the potentials, which form a hexagonal lattice as shown by the centers of the triangles in Fig. 2(a). We assume that there is one atom per each lattice site, and this atom interacts with the three neighbors in different directions through virtual tunneling with a potential barrier given by $V_0/4$.

In such a hexagonal lattice, we wish to engineer anisotropic Heisenberg exchange for each tunneling direction (denoted by D_x , D_y , and D_z , respectively). To this end, we apply three blue-detuned standing-wave laser beams in the X - Y plane along these tunneling directions:

$$V_{\nu\sigma}(x, y) = V_{\nu\sigma} \sin^2[k(x \cos\theta'_\nu + y \sin\theta'_\nu)], \quad (6)$$

where $\nu = x, y, z$, and $\theta'_x = -\pi/3$, $\theta'_y = \pi$, $\theta'_z = \pi/3$. In general, we require that the potential depth $V_{\nu\sigma}$ depend on the atomic spin state as

$$V_{\nu\sigma} = V_{\nu+} |+\rangle_\nu \langle +| + V_{\nu-} |-\rangle_\nu \langle -|, \quad (\nu = x, y, z), \quad (7)$$

where $|+\rangle_\nu$ ($|-\rangle_\nu$) is the eigenstate of the corresponding Pauli operator σ^ν with the eigenvalue $+1$ (-1).

The spin-dependent potentials in the form of Eqs. (6) and (7) can be realized, for instance, with the specific atomic level configuration shown in Fig. 2(c). Here, $\sigma = \uparrow, \downarrow$ denote two hyperfine levels of the atom with different energies. They are coupled to the common excited level $|e\rangle$ with a blue detuning Δ , respectively, through the laser beams L_1 and L_2 with frequencies matching the corresponding transitions. The quantization axis is chosen to be perpendicular to the X - Y plane, and the phase-locked laser beams L_1 and L_2 are both polarized along this direction. In the tunneling direction D_z , we only apply the L_1 laser beam, which induces the potential $V_{z\sigma}(x, y)$ with the desired form (7) of its depth $V_{z\sigma}$. In the tunneling direction D_x or D_y , we apply both lasers L_1 and L_2 , but with different relative phases, which realize the desired potential depth $V_{x\sigma}$ or $V_{y\sigma}$ of the form (7) in the corresponding direction.

The potentials (6) and (7) do not have influence on the equilibrium positions of the atoms, but they change the potential barrier between the neighboring atoms in the D_ν direction from $V_0/4$ to $V'_{\nu\sigma} = V_0/4 + V_{\nu\sigma}$. The parameters $V_{\nu+}$ and $V_{\nu-}$ in Eq. (7) can be tuned by varying the laser intensity of L_1 and L_2 in the D_ν direction, and one can easily find their appropriate values so that, in the D_ν direction, the atom can virtually tunnel with a rate $t_{+\nu}$ only when it is in the eigenstate $|+\rangle_\nu$. Hence, it follows from Eqs. (2) and (3) that the effective Hamiltonian for our system is given by Eq. (4) with $\lambda_\nu \approx -t_{+\nu}^2/(2U)$ for bosonic atoms with $U_\uparrow \approx U_\downarrow \approx U_1 \approx U$. After compensating effective magnetic fields, we find exactly the model described by the Hamiltonian (4).

The model (4) is exactly solvable due to the existence of many conserved operators, and it has been shown to possess very interesting properties [12]. In particular, it supports both Abelian and non-Abelian anyonic excitations, depending on the ratios between the three parameters λ_ν . In the region where $2\lambda_\nu/(\lambda_x + \lambda_y + \lambda_z) \leq 1$ ($\nu = x, y, z$), the excitation spectrum of the Hamiltonian (4) is gapless, but a gap opens when perturbation magnetic fields are applied in the x, y, z directions, and the excitations in this case obey non-Abelian fractional statistics. Out of this region, except at some trivial points with $\lambda_x\lambda_y\lambda_z = 0$, the Hamiltonian (4) has gapped excitations which satisfy Abelian fractional statistics. Thus, the present implementation opens up an exciting possibility to realize experimentally the exotic Abelian and non-Abelian anyons.

Now we briefly discuss the techniques for probing the resulting states. To detect the quantum phase transitions in the XXZ model with magnetic fields or in Kitaev's model, one can probe the excitation spectra via Bragg or Raman spectroscopy. In general, different quantum phases are characterized by specific dispersion relations (for instance, in Kitaev's model, one phase is gapped while the other is gapless). If the two probe light beams have the momentum and frequency differences which match those of the dispersion relation in the correspond-

ing phase, a resonant absorption of the probe light could be observed [21]. The direct observation of the fractional statistics in Kitaev's model can be based on atomic interferometry with a procedure similar to that described in Ref. [13]: One generates a pair of anyonic excitations with a spin-dependent laser focused on two lattice sites, rotates one anyon around the other, and then brings them together for fusion which gives different results depending on the anyonic statistics. Other methods for detecting complex quantum states of atoms have also been developed recently [22].

In summary, we have described a general technique to engineer many-body spin Hamiltonians.

We thank J. I. Cirac, D. DiVincenzo, W. Hofstetter, A. Kitaev, and P. Zoller for helpful discussions. This work was supported by NSF (EIA-0086038, DMR-0132874, and PHY-0134776), and by Sloan and Packard Foundations. L. M. D. also acknowledges support from the MURI Center DAAD19-00-1-0374, the CNSF, the CAS, and the "97.3" project 2001CB309300.

-
- [1] M. Greiner *et al.*, Nature (London) **415**, 39 (2002).
 - [2] C. Orzel *et al.*, Science **291**, 2386 (2001).
 - [3] D. Jaksch *et al.*, Phys. Rev. Lett. **81**, 3108 (1998).
 - [4] M. P. A. Fisher *et al.*, Phys. Rev. B **40**, 546 (1989).
 - [5] E. Demler and F. Zhou, Phys. Rev. Lett. **88**, 163001 (2002).
 - [6] K. Gross *et al.*, Phys. Rev. A **66**, 033603 (2002).
 - [7] W. Hofstetter *et al.*, Phys. Rev. Lett. **89**, 220407 (2002).
 - [8] A. B. Kuklov and B. V. Svistunov, Phys. Rev. Lett. **90**, 100401 (2003).
 - [9] A. Recati, P. O. Fedichev, W. Zwerger, and P. Zoller, Phys. Rev. Lett. **90**, 020401 (2003); B. Paredes and J. I. Cirac, Phys. Rev. Lett. **90**, 150402 (2003).
 - [10] A. Auerbach, *Interacting Electrons and Quantum Magnetism* (Springer-Verlag, New York, 1994).
 - [11] H. J. Briegel and R. Raussendorf, Phys. Rev. Lett. **86**, 910 (2001); **86**, 5188 (2001).
 - [12] A. Kitaev (to be published).
 - [13] B. Paredes *et al.*, Phys. Rev. Lett. **87**, 10402 (2001).
 - [14] A. C. Hewson, *The Kondo Problem to Heavy Fermions* (Cambridge University Press, Cambridge, England, 1997).
 - [15] See, e.g., E. A. Donley *et al.*, cond-mat/0204436.
 - [16] We note that, under the conditions of Ref. [1], an inhomogeneous Mott state can be created due to overall trapping potential. This can result in a domain structure involving new, coexisting phases, which will be discussed elsewhere.
 - [17] D. Jaksch *et al.*, Phys. Rev. Lett. **82**, 1975 (1999).
 - [18] O. Mandel *et al.*, cond-mat/0301169.
 - [19] G. K. Brennen *et al.*, Phys. Rev. Lett. **82**, 1060 (1999).
 - [20] M. E. Fisher and D. R. Nelson, Phys. Rev. Lett. **32**, 1350 (1974).
 - [21] W. Ketterle and S. Inouye, cond-mat/0101424.
 - [22] E. Altman, E. Demler, and M. D. Lukin, cond-mat/0306226.